

AUG 27 1997

CONF-970707--12

OSTI

HIGH EXPLOSIVE CORNER TURNING PERFORMANCE AND THE LANL MUSHROOM TEST

L.G. Hill, W.L. Seitz, C.A. Forest, & H.H. Harry

Los Alamos National Laboratory, Los Alamos, New Mexico 87545 USA

The Mushroom test is designed to characterize the corner turning performance of a new generation of less insensitive booster explosives. The test is described in detail, and three corner turning figures-of-merit are examined using pure TATB (both Livermore's Ultrafine and a Los Alamos research blend) and PBX9504 as examples.

INTRODUCTION

The use of insensitive high explosives in main charges has inevitably shifted safety concerns toward detonators and boosters. In particular, one would like to replace conventional HMX-based boosters with a less sensitive material. In response to this need Livermore has developed Ultrafine TATB (UF-TATB) and Los Alamos has developed PBX9504 (70 wt.% TATB, 25 wt.% PETN, 5 wt.% binder). These materials are less shock sensitive than conventional boosters, but the increased safety comes at a price. This is that less sensitive explosives have thicker reaction zones, and corner turning performance depends inversely on the product of the local wave curvature and the reaction zone width. Consequently, to maximize safety one must generally accept a booster material with marginal corner turning properties. Engineering design becomes critical, as one must decide how marginal the system can be given reasonable tolerances on factors like particle size, pressed density, and initial temperature. To make such decisions one needs a corner turning test optimized for the sensitivity of the materials in question. The Mushroom test is designed for this purpose.

All corner turning tests use the same basic idea: one delivers a small (modestly exceeding the failure diameter) but strong pressure stimulus* to

*This is opposite to an *initiation* test, which delivers a relatively large, weak, pressure stimulus to the sample.

the sample. The detonation then spreads with some difficulty, meaning that there is a large departure from ideal wave propagation (i.e., Huygen's construction) and a substantial "dead zone" in which detonation fails. The propagation of this marginal wave is quite sensitive to the material properties of the explosive, and the goal of a corner turning test is to characterize its departure from ideal propagation. Other than flash radiography (a useful but involved method), one must infer wavefront properties by observing detonation breakout from the test charge, and devise suitable figures-of-merit from these observations.

Besides being tuned for a particular class of explosives, the mushroom test has a few distinguishing features that set it apart from other corner turning tests (e.g., 1→3). One is that it uses a small amount of test explosive (about 8 gm), a virtue when material is scarce. Another is that it uses a hemispherical sample. This has several benefits: 1) the configuration is similar to that of real boosters, 2) the test samples the entire wavefront, which (assuming a constant detonation velocity) allows one to reconstruct its shape, and 3) the observation surface closely matches the shape of the emerging wave. The last attribute allows a very sensitive breakout measurement but, even more importantly, the angle between the emerging wave and the observation surface is always less than the critical angle, above which the presence of the latter affects the wave's shape.

DISCLAIMER

**Portions of this document may be illegible
in electronic image products. Images are
produced from the best available original
document.**

EXPERIMENTAL DETAILS

Figure 1 shows a scale drawing of the Mushroom test shot assembly. The test is named for its distinctive geometry—a 25.4 mm diameter pressed hemispherical “cap” of test material, initiated by a 6 mm-diameter × 24 mm-long “stem” composed of four PBX9407 (94 wt.% RDX, 6 wt.% binder) pellets. The stem’s purpose is to provide a strong and repeatable pressure input irrespective of the reproducibility of the Reynolds RP-2 detonator. Its 6 mm diameter was chosen by trial and error, using PBX9504 as the test explosive.

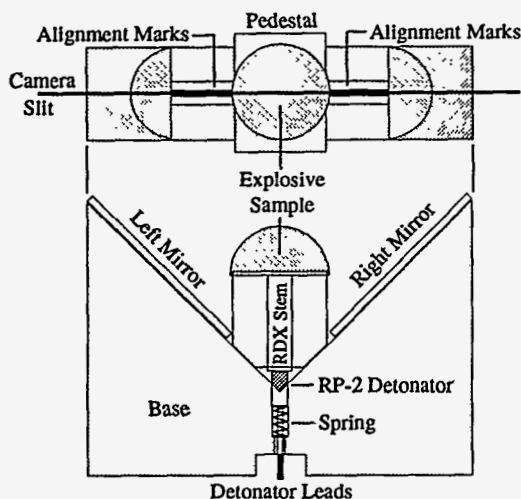


FIGURE 1. Scale drawing of the Mushroom Test

Samples are pressed directly to shape in a hemispherical die. Since the final volume is fixed, the sample density may be controlled simply by inserting the appropriate amount of mass. The bulk density of the finished pieces is also measured by immersion, as corner turning is quite sensitive to this parameter.

The sample is epoxied at four spots around the edges to a PMMA pedestal. The stem passes through a hole in the pedestal and contacts the equator of the test sample. The pedestal is epoxied to a PMMA base, which holds the detonator and two 45° mirrors. The detonator and pellets are spring-loaded against the test sample to ensure good contact between the pieces. The assembly is designed so that all pieces are automatically and accurately located with respect to one another.

Detonation breakout is observed with an internal-slit rotating mirror streak camera. The experiment is viewed directly and from two sides via the mirrors. The image of the camera slit spans the center of the hemisphere and its mirror images to give a composite streak record. The slit is precisely aligned by centering it between two blackened scribe marks on the pedestal (Fig. 1), which are visible in the mirror views. The sample surface is painted with aluminum fluosilicate to enhance the light output upon breakout.

Figure 2 shows a sample (negative) streak camera record. The two diagonal bands on top are the detonation wave traveling through the stem, as seen through the PMMA pedestal. Their termination indicates the entrance of the detonation wave into the pellet, and provides the time origin used for the breakout data. The three images on the bottom are detonation breakout and the subsequent product light from the three views.

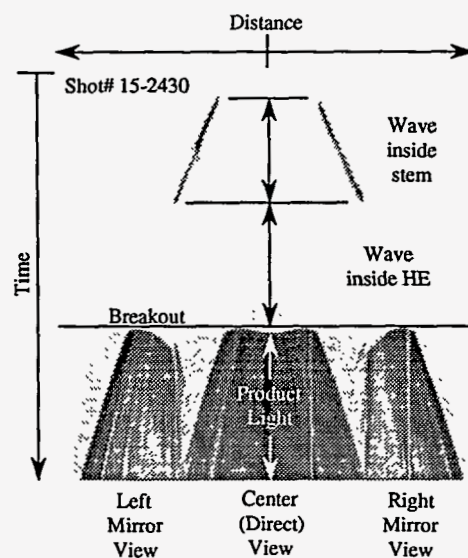


FIGURE 2. Mushroom test dynamic streak record.

The test is fired cold (-55 C) to observe worst case corner turning behavior. The shot is cooled at 1 C/min using dry nitrogen, and is soaked at temperature for 30 minutes. The styrofoam shot box has a double-glass observation window, and dry nitrogen is blown between the panes and also over the top pane to prevent condensation.

DATA REDUCTION

The streak records of Fig. 2 are digitized and combined to produce Fig. 3—a composite plot of breakout time vs. polar angle. For ideal propagation the wave would break out first at 90° because that path is the shortest. However, the real wave is retarded at larger angles because its strength is lower on the fringes. Consequently the wave breaks out at an intermediate angle first, giving the breakout plot its characteristic “w” shape.

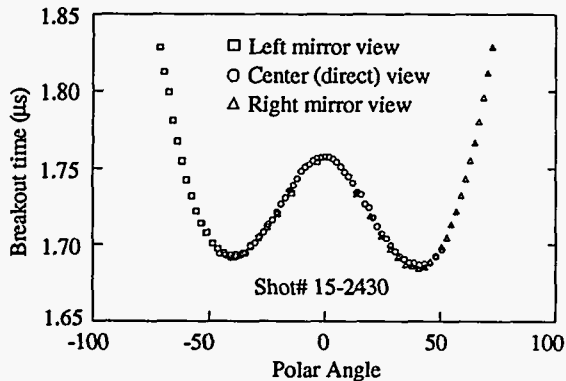


FIGURE 3. Composite breakout plot.

To achieve the level of consistency between the three views exhibited by Fig. 3 one must correct for certain experimental errors. The first is that one cannot distinguish in the dynamic record between the breakout locus and the edge of the detonation product cloud. Since breakout cannot extend beyond the undetonated charge, one may superimpose a still picture of the shot (not shown in Fig. 2) on the film above the dynamic record. The edges of the charge determined from it may then be used to “window out” spurious points.

Processing the data in this way one finds that the three views do not overlay to within the random scatter in the data. One reason is that the still and dynamic records are rarely in perfect alignment due, for example, to a slight amount of play in the mirror bearings. One may compensate for misalignment by laterally shifting the still picture (or rather, the “window” points it defines) relative to the dynamic record prior to processing the data. By trial and error one may then find an offset for which any remaining discrepancy between views is symmetric about the ordinate.

Having done so, one finds that the side and direct views agree in the vicinity of first breakout but deviate slightly near the pole and equator. This problem is closely related to the first; specifically, for sufficiently oblique angles the direct view observes the edge of the expanding product cloud rather than the breakout locus—and likewise for the mirror views. Thus, for angles greater than first breakout one should discard points from the direct view that deviate from those of the mirror views. Likewise, for angles less than first breakout one should discard points from the mirror views that deviate from those of the direct view.

ANALYSIS

The objective is to quantify how well the detonation spreads in a sample, compared to other samples tested under nominally identical conditions. For easy comparison it is desirable to distill the breakout plot of Fig. 3 into a single figure-of-merit. Regardless of how one defines such a quantity, it is beneficial to perform a series of tests at various pressed densities, and to plot the chosen figure-of-merit versus density. One may then fit a curve to the data and evaluate it at the nominal density. This is easier than pressing samples to exactly the nominal density; moreover, the curve's slope indicates the sensitivity of corner turning performance to density variations.

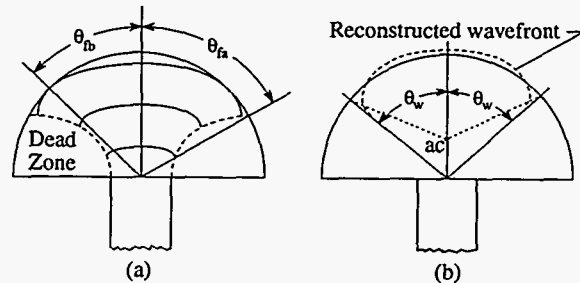


FIGURE 4. Definitions of First breakout angle and Failure angle (a), and Apparent center of initiation (b).

Three figures-of-merit are defined in Fig. 4. One is the first breakout angle θ_{fb} (Fig. 4a), corresponding to the two minima (averaged together) in Fig. 3. The better the wave spreads the less the lag at the edges, and the closer θ_{fb} is to the ideal 90° value. Fig. 5 shows data for PBX9504, UF-TATB, and a similar Los Alamos material, Fine-

particle TATB (FP-TATB). For each material θ_{f1} decreases linearly with pressed density. An inverse relationship is expected because less dense pressings have a larger internal void fraction, the collapse of which provides the mechanical work that initiates reaction.

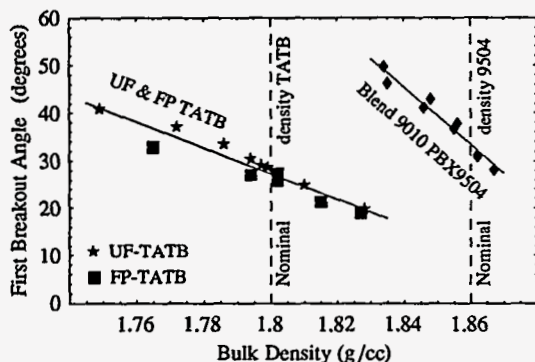


FIGURE 5. First breakout angle.

A second figure-of-merit (Fig. 4a) is the angle θ_{f1} at which the failure locus meets the observation surface. The failure locus separates the detonating region from the so-called "dead zone", and is indicated by an abrupt extinction of the breakout light (Fig. 2). Fig. 6 shows θ_{f1} for PBX9504, UF-TATB, and FP-TATB. For sufficiently low density θ_{f1} decreases linearly for all materials, but only the three highest density PBX9504 samples had θ_{f1} 's less than the maximum value of 90°. For the both TATB materials θ_{f1} rolls off exponentially starting at about the nominal density of 1.8 g/cc. For sufficiently high densities PBX9504 may do the same, but it differs from pure TATB in that it is sensitized by PETN rather than void space.

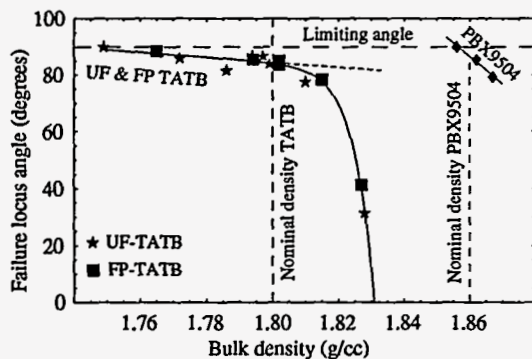


FIGURE 6. Failure locus angle.

The third figure-of-merit presented is derived from wavefront reconstruction. The emerging wave shape may be calculated (Fig. 4b) given the shape of the observation surface and assuming the wave speed to be curvature-independent. A circle is fit to the reconstructed wave at the mean breakout time, in a chosen angular window θ_w . Its center relative to the geometric center of the sample, Y_{ac} , is the *apparent center of initiation*. If the wave expansion is close to spherical then $|Y_{ac}|$ is small, but if spreading is poor the apparent center moves up into the sample.

Figure 7 shows Y_{ac} for PBX9504, UF-TATB, and FP-TATB. The detonation velocity for each material lot was taken to be the ratio of the sample height to centerline transit time, averaged over all the samples in the lot. In each case the angular window is chosen to be equal to the failure angle. It is seen that Y_{ac} increases linearly with density except for the two highest TATB densities, for which it decreases. It is clear from Fig. 6 that this reversal does not indicate improved corner turning, but is a peculiarity of the failing wave.

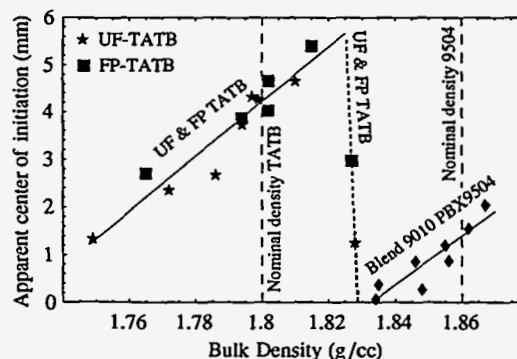


FIGURE 7. Apparent center of initiation.

ACKNOWLEDGEMENTS

We thank A. Anderson for contributing to the analysis, and G. Vasilik & D. Murk for firing support. This work was supported by the U.S. DOE.

REFERENCES

1. Cox, M., and Campbell, A.W., 7th Symp. (Int.) on Detonation (1981).
2. Forbes, J.W., Lemar, E.R., and Baker, R.N., 9th Symp. (Int.) on Detonation (1989)
3. Hutchinson, C.D., Foan, G.C.W., Lawn, H.R., and Jones, A.G., 9th Symp. (Int.) on Detonation (1989)

DISCLAIMER

This report was prepared as an account of work sponsored by an agency of the United States Government. Neither the United States Government nor any agency thereof, nor any of their employees, makes any warranty, express or implied, or assumes any legal liability or responsibility for the accuracy, completeness, or usefulness of any information, apparatus, product, or process disclosed, or represents that its use would not infringe privately owned rights. Reference herein to any specific commercial product, process, or service by trade name, trademark, manufacturer, or otherwise does not necessarily constitute or imply its endorsement, recommendation, or favoring by the United States Government or any agency thereof. The views and opinions of authors expressed herein do not necessarily state or reflect those of the United States Government or any agency thereof.